Arabian Journal of Chemistry (2017) **10**, S472–S483

King Saud University

Arabian Journal of Chemistry

www.ksu.edu.sa
www.sciencedirect.com

ORIGINAL ARTICLE

Spectroscopic, electrochemical and biological studies of the metal complexes of the Schiff base derived from pyrrole-2-carbaldehyde and ethylenediamine

Bibhesh K. Singh [a,*], Parashuram Mishra [b], Anant Prakash [a], Narendar Bhojak [c]

[a] *Department of Chemistry, Govt. Post Graduate College, Ranikhet 263645, Uttarakhand, India*
[b] *Bioinorganic & Material Chemistry Laboratory, Tribhuvan University, MMAM Campus, Biratnagar, Nepal*
[c] *Department of Chemistry, Govt. Dunger College, MGS University, Bikaner, Rajasthan, India*

Received 21 July 2011; accepted 14 October 2012
Available online 1 November 2012

KEYWORDS

Electrochemical studies;
Metal complex;
Molecular modeling;
Schiff base;
Spectra

Abstract The new symmetrical Schiff base *N*,*N*′bis(pyrrole-2-carbaldehyde)ethylenediamine and its Mn(II), Co(II), Ni(II) and Cu(II) complexes were synthesized and characterized by spectral, magnetic and electrochemical studies. The spectral studies of the complexes reveal that the ligand has coordination through the azomethine nitrogen atoms, pyrrole nitrogen atoms and anions, supported by octahedral geometry. Mass spectrum explains the successive degradation of the molecular species in solution and justifies ML complexes. The electrochemical study indicates that the pyrrole ring stabilizes the metal ion, makes the complex more positively charged, and causes it to be more easily reduced. The molecular structure of the complexes has been optimized by MM2 calculations and suggests an octahedral geometry. Powder X-ray diffraction allows us to determine the cell parameters of the complexes. The bio-efficacy of the ligand and their complexes has been examined against the growth of bacteria in vitro to evaluate their anti-microbial potential.

1. Introduction

A combination of distinctly different metal ion binding sites within one ligand can lead to materials with interesting new properties such as specific sensors, molecular wires, magnetic and optical devices (Parekh and Patel, 2006). The flexibility of Schiff base ligands can be improved by hydrogenation of their C═N bonds; they should thus coordinate metal ions more easily. For these reasons, reduced Schiff bases have recently gained considerable attention (Belaid et al., 2008). Schiff base metal complexes attract considerable interest and occupy

* Corresponding author. Tel.: +91 9760014796; fax: +91 5966220372.
E-mail address: bibheshksingh@yahoo.co.in (B.K. Singh).
Peer review under responsibility of King Saud University.

ELSEVIER Production and hosting by Elsevier

http://dx.doi.org/10.1016/j.arabjc.2012.10.007
1878-5352

an important role in the development of the chemistry of chelate systems due to the fact that especially those with N_2O_2 or N_4 tetradentate ligands, closely resemble metallo-proteins (Abd El-Wahab and El-Sarrag, 2004; Anacona et al., 2009; Bezaatpour et al., 2011; Firdaus et al., 2010). On the other hand, different metal complexes with a wide variety of Schiff bases having such tetradentate donor atoms around the metal ion have been used as catalysts for epoxidation, hydroformylation, hydrogenation, electrochemical investigation and biological studies of proteins (Abd El-Wahab and El-Sarrag, 2004; Anacona et al., 2009; Bezaatpour et al., 2011; Firdaus et al., 2010). The development in the field of bioinorganic chemistry has been another important factor in spurring the growth of interest in macrocyclic compounds (Valencia et al., 2001; Yang et al., 2009; Raman et al., 2009). Chemically macrocycle containing moieties are of great interest because of their great versatility as ligands, due to the presence of several potential donor atoms, their flexibility and ability to coordinate in either neutral or deprotonated form (Valencia et al., 2001; Yang et al., 2009; Raman et al., 2009; Uysal and Kursunlu, 2011). Many transition metal ions in living systems work as enzymes or carriers in a macrocyclic ligand environment. Meaningful research in this direction might generate simple models for biologically occurring metalloenzymes (Saleh, 2005; Kumar and Alexander, 1999). The behavior of the >C═N bond is strongly dependent on the structure of the amine moiety, which in turn controls the efficiency of the conjugation and may incorporate structural elements able to modulate the steric crowding around the coordination. Various studies have shown that the >C═N group has considerable biological importance (Gudasi et al., 2006).

During the last decade, the coordination chemistry of Schiff bases derived from heterocyclic carbaldehyde has received much attention (Alvarez et al., 2007; Ray et al., 2008; Mohamed et al., 2005; Singh et al., 2010). Recently the stability of N_4 tetradentate Schiff bases in the presence of Sm(II) reagent, determined by the introduction of a pyrrole ring able to coordinate to Sm(II) ion has been studied (Berube et al., 2003). Encouraged by these reports, we have synthesized and characterized the new symmetrical Schiff base *N*,*N*′ bis(pyrrole-2-carbaldehyde) ethylenediamine and its metal complexes.

2. Experimental

All the chemicals used were of analytical grade and were used as procured. The reagent grade chemicals pyrrole – 2-carbaldehyde, ethylenediamine, tetrabutylammonium perchlorate (n-Bu_4 $NaClO_4$) and metal salts were purchased from Aldrich and Fluka Chemicals Co. and used without further purification. The elemental analyses(C, H and N) of the complexes were performed using Elementar vario EL III model. Metal contents were estimated on an AA-640-13 Shimadzu flame atomic absorption spectrophotometer in solutions prepared by decomposing the complexes in hot concentrated HNO_3. The molar conductivities of complexes have been measured using a Sybron–Barnstead conductometer in DMSO of 10^{-3} M of their solutions at room temperature. The IR spectra were recorded on a Spectrum BX II model Perkin–Elmer FTIR spectrophotometer in KBr and polyethylene pellets in the range 400–4000 cm^{-1} and 100–400 cm^{-1}, respectively. The UV–visible spectra were recorded in DMSO on Beckman DU-64 spectrophotometer with quartz cells of 1 cm path length from 200–900 nm and mass spectra (TOF-MS) were recorded on Waters KC-455 model with ES^+ mode in DMSO. ^1H NMR spectra were recorded in DMSO-d_6 solvent on a Bruker Avance 400 MHz instrument. X-band EPR spectra was recorded on a Varian E-112 spectrometer with a variable temperature liquid nitrogen cryostat (The error in g value is ± 0.001) and g factors were quoted relative to the standard marker tetracynoethylene (TCNE, $g = 2.00277$). Cyclic voltametric measurements were carried out with a PC-controlled Eco Chemie-Autolab-12 potentiostat/galvanostat electrochemical analyzing system at 27 °C in a three-electrode cell using nitrogen purged DMSO solution containing 0.1 M tetrabutylammonium perchlorate (TBAP) and 10^{-3} M of the complex, in the potential range −1.0 to +2.0 V. A Pt wire is used as a working electrode and Ag/AgCl as a reference electrode. Magnetic susceptibility measurements were carried out at room temperature in powder form on a vibrating sample magnetometer PAR 155 with 5000G-field strength, using $Co[Hg(SCN)_4]$ as the calibrant(magnetic susceptibility $\approx 1.644 \times 10^{-5}$ cm^3g^{-1}). Rigaku model 8150 thermoanalyser was used for simultaneous recording of TG–DTA curves at a heating rate of 10 min^{-1}. For TG, the instrument was calibrated using calcium oxalate, while for DTA, calibration was done using indium metal, both of which were supplied along with the instrument. A flat bed type aluminum crucible was used with α-alumina (99% pure) as the reference material for DTA. The XRD powder pattern was recorded on a vertical type Philips 1130/00 diffractometer, operated at 40 kV and 50 Ma generator using the monochromatized Cukα line at wavelength 1.54056 Å as the radiation sources. Sample was scanned between 10° and 70° (2θ) at 25 °C. The crystallographic data were analyzed by using the CRYSFIRE – 2000 powder indexing software package and the space group was found by GSAS program. Debye Scherer relation in conjunction with an estimation of 100% peak width was used to estimate the particle size. The density was used to estimate the particle size. The density was determined using Archimedes method.

2.1. Synthesis of ligand and metal complexes

2.1.1. Synthesis of *N*,*N*′-bis(pyrrole-2-carbaldehyde) ethylenediamine (Ligand)

Pyrrole-2-carbaldehyde (40 mmol) was dissolved in absolute ethanol (30 ml) added dropwise to a solution of ethylenediamine (20 mmol) in absolute ethanol (30 ml) with constant stirring. Stirring was continued with heating at 60 °C for 2 h. A skin colored crystalline powder was collected by vacuum filtration and dried overnight in vacuum.

2.1.2. Synthesis of metal complexes

N,*N*′-Bis(pyrrole-2-carbaldehyde) ethylenediamine (10 mmol) in 20 ml of absolute ethanol was added dropwise to a solution containing metal salts (10 mmol) in absolute ethanol (20 ml). The mixture was refluxed for 4–6 h on water bath. The precipitate was filtered, washed with cold alcohol and dried under vacuum over silica gel. The metal salts used were Manganese chloride, cobalt nitrate, nickel acetate and copper acetate.

2.2. Molecular modeling

3D molecular modeling of the proposed structure of the complexes was performed using CsChem3D Ultra-11 program

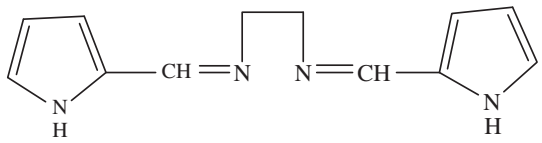

Figure 1 Structure of the ligand.

package. The correct stereochemistry was assured through the manipulation and modification of the molecular coordinates to obtain reasonable low energy molecular geometries. The potential energy of the molecule was the sum of the following terms (E) = E_{str} + E_{ang} + E_{tor} + E_{vdw} + E_{oop} + E_{ele}, where all Es represent the energy values corresponding to the given types of interaction (kcal/mol). The subscripts str, ang, tor, vdw, oop and ele denote bond stretching, angle bonding, torsion, deformation, vanderwaals interactions, out of plain bending and electronic interaction, respectively. The molecular mechanics describe the application of classical mechanics to the determination of molecular equilibrium structures. It enables the calculation of the total static energy of a molecule in terms of deviations from reference unstrained bond lengths, angles and torsions plus non-bonded interactions. On account of non-bonded interactions and also the chemical sense of each atom, treat the force field as a set of constants that have to be fixed by appeal to experiment or more rigorous calculations. It has been found that off-diagonal terms are usually largest when neighboring atoms are involved, and so we have to take account of non-bonded interactions, but only between next-nearest neighbors.

2.3. Biological activity: antibacterial screening

In vitro antibacterial activity of the compounds against *Escherichia coli* and *Staphylococcus aureus* was carried out using Muller–Hinton Agar media (Hi media). The activity was carried out using a paper disc method. Base plates were prepared by pouring 10 ml of autoclaved Muller–Hinton agar into sterilized petri dishes (9 mm diameter) and allowing them to settle. Molten autoclaved Muller–Hinton that had been kept at 48 °C was incubated with a broth culture of *E.* coli and *S.* aureus bacteria and then poured over the base plate. The discs were air dried and placed on the top of agar layer. The plates were incubated for 24–30 h and the inhibition zones (mm) were measured around each disc. As the organism grows, it forms a turbid layer, except in the region where the concentration of antibacterial agent is above the minimum inhibitory concentration, and a zone of inhibition is seen. The solutions of all compounds were prepared in double distilled water and chloramphenicol was used as a reference.

3. Results and discussion

The synthesized compounds are crystalline colored, non-hygroscopic, insoluble in water, partially soluble in ethanol but soluble in DMF and DMSO. The coordination of the metal to the tetradentate ligand (Fig. 1) is obtained by two N atoms of azomethine group and two N atoms of pyrrole ring. Composition and identity of the assembled system were deduced from elemental analysis (Table 1) and spectroscopic studies (IR, UV–Vis, ^{1}H NMR, EPR, Mass), magnetic and electrochemical studies. The results of the elemental analyses of the complexes in Table 1 are in good agreement with those required by the proposed formulae. In all cases 1: 1(M:L) solid complexes are isolated and found to have the general formula $[MLX_2]$. nH_2O where M = Mn(II), Co(II), Ni(II) and Cu(II) when X = Cl^- or NO_3^- or CH_3COO^- and n = 0–1. The lattice water molecules have been determined with the help of elemental as well as thermal studies. The TG–DTA was carried out for metal complexes in ambient conditions (Fig. 2). The correlations between the different decomposition steps of the complexes with the corresponding weight losses have been studied. The first estimated mass loss within the temperature range 315–360 K may be attributed to the loss of water molecules in complexes I, II and IV. This dehydration range indicates the presence of non-coordinated water molecule in the complex. That the DTA curve gives an endothermic peak within the temperature range of 322–355 K also confirms this fact. The conductance measurements show these complexes to be non-electrolytes and the mass spectra determinations indicate their monomeric nature. Single crystal of the compounds could not be isolated from any organic solvents; thus Powder X-ray diffraction helps to predict crystal system. However, the analytical and spectroscopic data enable us to predict possible structures.

3.1. Spectroscopic and magnetic studies

The ^{1}H NMR spectrum of the ligand (Fig. 3) in DMSO showed a singlet at δ 9.40 ppm, has been assigned to the azomethine proton (HC═N). The peaks in the regions δ

Table 1 Color, reaction yield and elemental analysis of the ligand and complexes.

S. No.	Compound/complex (empirical formula)	Color	Conductance (ohm^{-1} mol^{-1} cm^2)	Yield (%)	Elemental analysis found/(calc.) (%)				μ_{eff} (BM)
					C	H	N	M	
1	Ligand (L) ($C_{12}H_{14}N_4$)	Skin colored	–	88	67.21 (67.28)	6.50 (6.54)	26.14 (26.16)	– –	–
2	$[MnLCl_2]\cdot H_2O$ (I) ($MnC_{12}H_{16}N_4OCl_2$)	Brown	10	86	40.22 (40.24)	4.42 (4.47	15.62 (15.64)	15.31 (15.35)	5.95
3	$[Co(L)(NO_3)_2]\cdot H_2O$ (II) ($CoC_{12}H_{16}N_6O_7$)	Black	8	82	34.67 (34.70)	3.87 (3.85)	20.27 (20.24)	14.17 (14.20)	4.80
4	$[Ni(L)(CH_3COO)_2]$ (III) ($NiC_{16}H_{20}O_4N_4$)	Dark brown	14	84	49.15 (49.14)	5.09 (5.11)	14.31 (14.33)	15.00 (15.02)	2.78
5	$[Cu(L)(CH_3COO)_2]\cdot H_2O$ (IV) ($CuC_{16}H_{22}O_5N_4$)	Blue	12	86	46.40 (46.42)	5.30 (5.31)	13.52 (13.54)	15.30 (15.36)	1.80

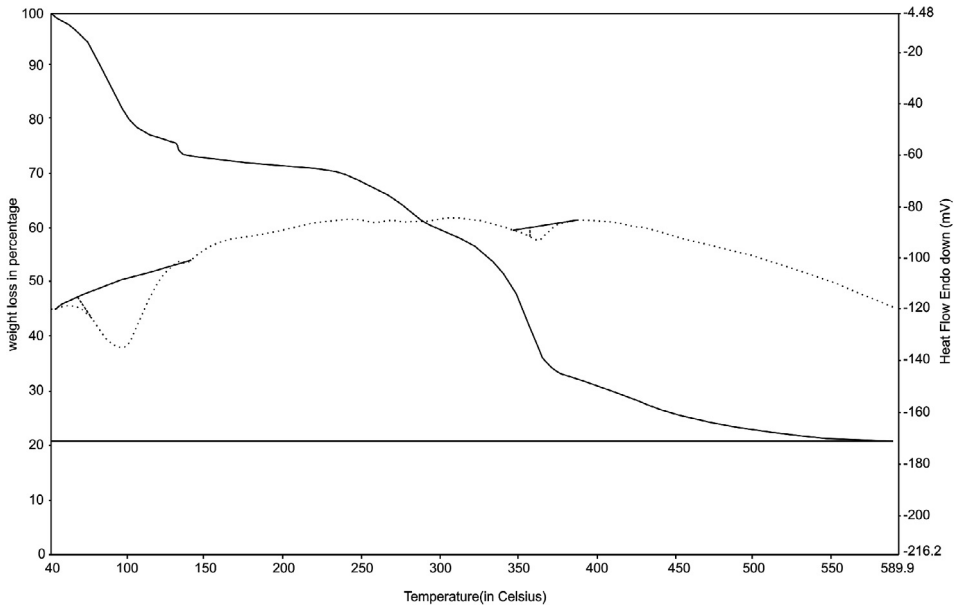

Figure 2 TG/DTA curve of complex IV.

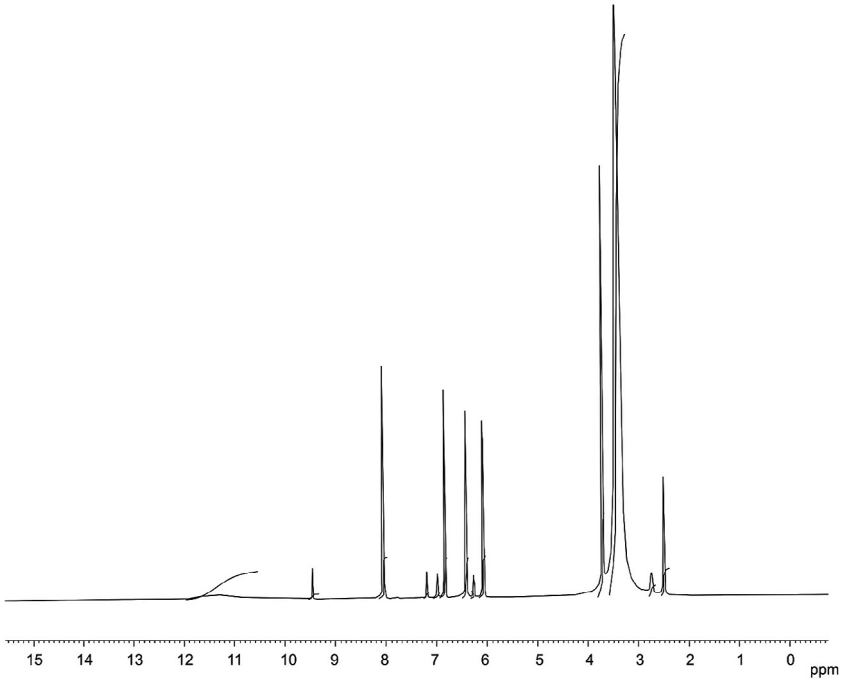

Figure 3 ^{1}H NMR spectrum of the ligand.

7.1–8.1 ppm were assigned chemical shifts for the hydrogen of the symmetrical aromatic ring of the ligand. Protons on the methylene group attached to a nitrogen atom, N–CH_2–, with resonances in the region of δ 3.40–3.90 ppm as singlet pattern (Aranha et al., 2007; Kasumov et al., 2005). The peaks in the region δ6.0–6.9 ppm were assigned to a chemical shift of pyrrole hydrogen and a singlet peak at δ 11.60 ppm due to NH of pyrrole ring (Silverstein and Webster, 2007). Metal complexes are paramagnetic; their ^{1}H NMR spectra could not be obtained.

Mass spectrometry has been successfully used to investigate molecular species in solution (Sanmartin et al., 2006; Beloso et al., 2003; Singh et al., 2009). This method is particularly useful when a poorly crystalline nature of complexes prevents their X-ray characterization. The pattern of mass spectrum (Fig. 4a–c) gives an impression of the successive degradation of the target compound with the series of peaks corresponding to the various fragments. Their intensity gives an idea of stability of fragments. The recorded molecular ion peaks of the metal complexes have been used to confirm the proposed formula.

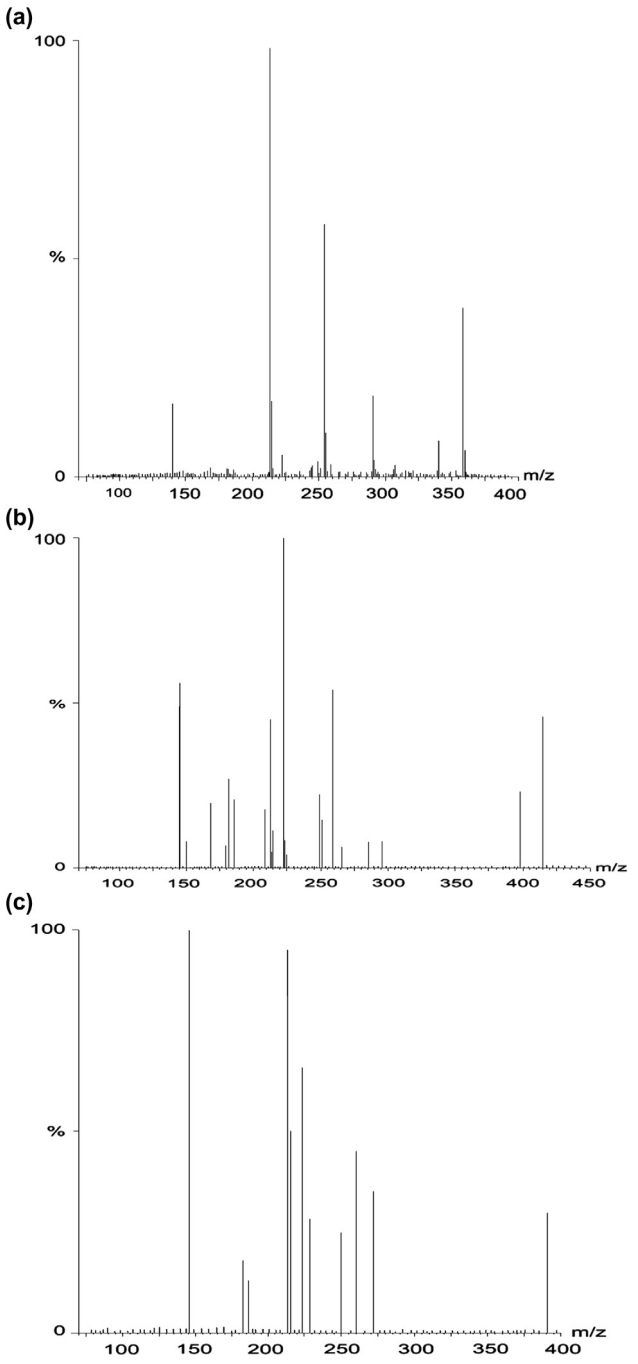

Figure 4 (a) Mass spectrum of complex I. (b) Mass spectrum of complex II. (c) Mass spectrum of complex III.

The mass spectrum of the ligand having a molecular ion peak at 214{100% *m*/*z*} and having a prominent peak at 145{73% *m*/*z*} that corresponds to the $[C_9H_8NO]^+$ confirms the purity of the ligand. The molecular ion peaks of Mn(II), Co(II), Ni(II) and Cu(II) – Schiff base complexes were observed at 358, 415, 391 and 414 *m*/*z* respectively, which confirm the stoichiometry of the metal complexes to be $[M(L)(X)_2]\cdot nH_2O$. All the synthesized complexes containing metal ion were confirmed by good agreement between the observed and calculated molecular formula (Swamy and Pola, 2008). Elemental analysis values are in close agreement with the values calculated from molecular formulae assigned to these complexes, which is further supported by the TOF–mass studies. The molecular ion peak of the complexes by the loss of water molecules gave a fragment ion $[M(L)(X)_2]^+$. All these fragments leading to the formation of the monomeric species $[M(L)]^+$ which undergo demetallation to form the species $[HL]^+$ are usually present in the mass spectra of these systems (Yoshida et al., 2000).The last two fragments at 214 and 146/145 are $[LH]^+$ and $[C_9H_8NO]^+$ of ligand peaks appearing in all the complexes showing a similar pattern of degradation.

The existence of numerous coordination sites in the ligand give variable binding modes, however, comparison of the infrared spectrum of the ligand and its complexes revealed that the ligand is bonded to metal ions in a quadridentate mode. The significant IR bands of the Schiff base and its metal complexes are given in Table 2. The free Schiff base ligand showed a strong band at 1641 cm^{-1} which is characteristic of the azomethine (HC═N–) group (Ramesh and Maheshwaran, 2003). Coordination of the Schiff base to the metal ions through the nitrogen atom is expected to reduce electron density in the azomethine link and lower the $\nu_{C=N}$ absorption frequency. The band due to $\nu_{C=N}$ is shifted to lower frequencies and appears in the range of 1610–1625 cm^{-1}, indicating coordination of the azomethine nitrogen to metal ions (Keypour et al., 2009). The coordination of the azomethine nitrogen is further supported by the appearance of bands in the range of 460–530 cm^{-1} due to $\nu_{C=N}$. The N–H stretching frequency at 3109 cm^{-1} in the free ligand showed a considerable shift in all the complexes, indicating participation of this N–H group in complexes (Kumar et al., 2003). In complex I, the ν(Mn–Cl) band is observed at 364 cm^{-1} which showed terminal rather than bridging chlorine (Nakamoto, 1978). In addition on account of the slightly modified coordination, infrared spectra of complex II show absorption bands at ca. 1265, 1090, 735, 1378, 960, 1030 cm^{-1} due to coordinated nitrato group. These bands are assigned as ν_1, ν_2, ν_3, ν_4, ν_5, ν_6 modes respectively, and their frequencies are consistent with those associated with terminally bonded monodentate nitrato group (Addison and Sultons, 1967; Addision et al., 1971). In addition to these two weak bands with a separation of ca. 14 cm^{-1} appear in the 1800–1700 cm^{-1} region indicating clearly the exclusive presence of terminal monodentate nitrato group (Lever et al., 1971; Choca et al., 1972). Complexes III and IV have bands in the regions of 1615–1625 and 1403–1411 cm^{-1} which can be assigned to $\nu_{as}(CO_2)$ and $\nu_s(CO_2)$ fundamental stretching bands respectively, which are in agreement with the acetate groups being monodentate and indicating the covalent nature of metal oxygen bond (Nakamoto, 1978). Complexes I, II and IV showed a broad band in the region of 3422–3502 cm^{-1} due to (OH) from water molecules present out side the coordination sphere as lattice. This has been confirmed with thermal studies. These bands are absent in the ligand.

The electronic spectra of ligand and its metal complexes were recorded in DMSO. The spectrum of ligand consists principally of one band at ca. 23148 cm^{-1} due to $n\rightarrow\pi^*$ transition of the azomethine group and is shifted to a longer wavelength on coordination through azomethine nitrogen (Prakash et al., 2010). The electronic spectra of the Mn(II) complex exhibit four weak intensity bands at 19280, 23265, 28260 and 38528 cm^{-1}. These bands may be assigned to the transitions, $^6A_{1g} \rightarrow {}^4T_{1g}$ (^4G), $^6A_{1g} \rightarrow {}^4E_g$, $^4A_{1g}$ (^4G), $^6A_{1g} \rightarrow {}^4E_g$ (D), and $^6A_{1g} \rightarrow {}^4T_{1g}$ (^4P) respectively, which lie in

Table 2 Infrared spectral data (cm^{-1}) of ligand and complexes.

S. No.	Compound/complex	ν(C=N)	ν(M–N)	ν(M–O)	ν(M-Cl)	ν(NO_3)	$\nu_{as}(CO_2)$	$\nu_S(CO_2)$
1	L	1641(s)	–	–	–	–	–	–
2	I	1625(s)	530(m)	–	364(m)	–	–	–
3	II	1620(s)	523(m)	563(m)	–	1265(ν_1), 1090(ν_2), 735(ν_3), 1378(ν_4), 960(ν_5), 1030(ν_6)	–	–
4	III	1610(s)	520(w)	560(m)	–	–	1615(m)	1403(s)
5	IV	1618(s)	468(m)	501(m)	–	–	1625(s)	1411(s)

s: strong, m: medium, w: weak.

the same range as reported for octahedrally coordinated Mn(II) ion (Kumar and Chandra, 2007). The ground state of the d^5 system in a weak octahedral field has the spins of the d orbital which are parallel, making it a spin sextuplet. This, however, is the only sextuplet state possible, for every conceivable alteration of the electron distribution $t_{2g}^3e_g^2$ results in the pairing of two or four spins, thus making quartet or doublet states. Hence, all excited states of the d^5 system have different spin multiplicity from the ground state, and transitions to them are spin forbidden. Because of weak spin–orbit interactions, such transitions are not totally absent, but they give rise only to very weak absorption bands. The magnetic moment 5.95 BM is an additional evidence for an octahedral structure of the Mn(II) complex (Figgis, 1978; Carlin, 2002; Cotton and Wilkinson, 1972). For Co(II) complex, three spin allowed transitions are: $^4T_{1g}$ (F) → $^4T_{2g}$ (F) (ν_1) (8412 cm^{-1}), $^4T_{1g}$ (F) → $^4A_{2g}$ (F) (ν_2) (≈18,000 cm^{-1}) and $^4T_{1g}$ (F) → $^4T_{1g}$ (P) (ν_3) (21302 cm^{-1}) (Kandaz et al., 2002). The first band appeared at 8412 cm^{-1} usually in the infrared region, so ν_1 transition due to $^4T_{1g}$ (F) → $^4T_{2g}$ (F) could not be observed in the complex. The second transition is two electronic processes and therefore their bands are of low intensity. The broad band with maximum at 21302 cm^{-1} corresponds to the highest energy $^4T_{1g}$ (F) → $^4T_{1g}$ (P) transition. The room temperature magnetic moment for Co(II) complex is 4.80 BM that supports an octahedral complex (Omar and Mohamed, 2005). Electronic spectra of six coordinated Ni(II) complex may possesses either O_h or D_{4h} symmetry. The Ni(II) complex exhibits three d-d transition bands for the transitions: $^3A_{2g}$ → $^3T_{2g}$ (F) (ν_1) (9732 cm^{-1}), $^3A_{2g}$ → $^3T_{1g}$ (F) (ν_2) (14198 cm^{-1}) and $^3A_{2g}$ → $^3T_{1g}$ (P) (ν_3) (21340 cm^{-1}) (Ahamed et al., 2008). The magnetic moment of the Ni(II) complex at room temperature lies at 2.78 B.M. corresponds to two unpaired electrons, and is consistent with a weak field octahedral geometry as expected. However, this magnetic moment value is lower than the spin only value for two unpaired electrons in the nickel(II) complex, indicative of some antiferromagnetic behavior (Ranford et al., 1993). The electronic spectra of six coordinated copper(II) complex (^2D free ion) will split into B_{1g}, A_{1g}, B_{2g} and E_g levels, respectively. Thus three spin allowed transitions are expected in the visible and near IR region, but only a few examples are known, in which such bands are resolved (Figgis and Lewis, 1964; Chandra and Sharma, 2002). These bands have been assigned to the following transitions in order of increasing energy, $^2B_{1g}$ → $^2A_{1g}$ (dz^2 → dx^2-y^2), $^2B_{1g}$ → $^2B_{2g}$ (dxy → dx^2-y^2) and $^2B_{1g}$ → ^2E_g ($d_{xz,yz}$ → dx^2-y^2). The energy level sequence will depend on the amount of tetragonal distortion due to ligand field and Jahn–Teller effects (Lever, 1984; Wang et al., 2003; Tomilson et al., 1965). The electronic absorption spectra recorded in the range of 25,000–11,112 cm^{-1} show a broad absorption band (λ_{max} = 17361 cm^{-1}). It is difficult to assign the transition of this band because it is due to mixing of all transitions. The magnetic moment of the copper complex is 1.80 BM which confirms octahedral arrangement.

EPR spectrum of the Mn(II) complex(High spin Mn(II) having ground state term $S_{5/2}$) was recorded at room temperature in DMSO solution and $g_{\|}$ (3.78), $g_{\perp}$ (1.92), A_0 (103) and g_{iso} (2.70) values were calculated. The combined action of spin–spin interaction and electric field gradient produces splitting of the energy levels due to second order spin orbit coupling between the A_{1g} ground state and the lowest level of the $^4A_{2g}$ state (Jorgensen, 1969). Since d^5 is an odd electron system whose ground state is a Kramer's doublet and whose degeneracy is only completely removed by a magnetic field, a resonance is readily detected even for large zero field splitting. The Mn(II) complex gives epr spectra containing the six lines arising due to the hyperfine interaction between the unpaired electron with the ^{55}Mn nucleus(I = 5/2). The nuclear magnetic quantum numbers, corresponding to these lines are −5/2, −3/2, −1/2, +1/2, +3/2 and +5/2 from low to high field (Jorgensen, 1969). The copper(II) ion, with d^9 configuration, has an effective spin of S = 1/2 and is associated with a spin angular momentum, m_s = ±1/2 leading to a doubly degenerate spin state in the absence of magnetic field. In a magnetic field the degeneracy is lifted between these states and the energy difference between them is given by E = hν = gβH, where h is Planck's constant, ν is the microwave frequency for transition from ms = + ½ to − ½, g is the Lande splitting factor (equal to 2.0023 for a free electron), β is the Bohr magneton and H is the magnetic field. The epr spectrum of polycrystalline sample of Cu(II) at Liquid nitrogen temperature gives three g values($g_3 > g_2 > g_1$) which indicate rhombic distortion is very small. The geometric parameter G, which is a measure of the exchange interaction between the copper centers in the polycrystalline compound, is calculated using the equation: $G = (g_{\|} - 2.0023)/(g_{\perp} - 2.0023)$ for axial spectra and for rhombic spectra $G = (g_3 - 2)/(g_{\perp} - 2)$ and $g_{\perp} = (g_1 + g_2)/2$. If G > 4, exchange interaction is negligible if it is less than four; considerable exchange interaction is indicated in the solid complex (Hathaway and Billing, 1970). The lowest g > 2.04, a spectrum can be observed for a copper(II) ion in elongated rhombic symmetry with all the axes aligned parallel and would be consistent with elongated rhombic–octahedral complexes (Hathaway and Billing, 1970). In the complex, $g_{\|} > g_{\perp} > 2.0023$ and G value within the range 2.08–4.49 are consistent with dx^2-y^2 ground state (Bew et al., 1972). From the observed g values it is evident that the unpaired electron lies predominantly in the dx^2-y^2 orbital with a possibility of some dz^2 character being mixed with it because of low symmetry. The shape of ESR lines indicates that the

present complex may have octahedral geometry. In the complex, $g_{\|} < 2.3$ was observed and it indicates a fair degree of covalent character in the Cu–L bonding (Kivelson and Neiman, 1968).

3.2. Electrochemical studies

The present study is focused on the redox behavior of the Schiff base – Mn(II), Co(II), Ni(II) and Cu(II) – chelates, where the electron acceptor and electron donating properties of the ligand were reflected in the electrochemical properties. The influence of the substituent in the Schiff base moiety on the stability of above complexes was also investigated. The cyclic voltametric profile of the Mn(II) complex (Fig. 5) reveals the presence of an irreversible, anodic process ($E_p = +0.79$ V) and quasi-reversible reduction($E_{1/2} = -1.06$ V), which regenerates in the reverse scan of the oxidation of the original complex. On this basis, the oxidation may be attributed to the Mn(II)/Mn(III) couple, where the Mn(III) complex after its formation, being quite unstable in the original geometry, evolves to an unidentified differently coordinated species (fragmentation cannot be ruled out), which, however upon reduction regenerates the Mn(II) complex. The cyclic voltametric profile of the cobalt complex, displayed irreversible one-electron reduction in DMSO containing a Ag/AgCl electrode system with a peak separation value ($\Delta E_P = 0.224$ V). The reduction wave could be assigned to metal-based Co(III)/Co(II) couples in the complex. The cathodic peak potential of the complex is located at $E_{pc} = -0.740$ V verses Ag/AgCl (Yilmaz and Kocak, 2004; Yilmaz et al., 2005; Kandaz et al., 2002). The nickel complex shows two oxidation processes. The first one is irreversible ($\Delta E_{P1} = 0.28$ V) and may be attributed to the oxidation of ligand. The second one is reversible ($\Delta E_{P2} = 0.09$ V) and consistent with a one-electron oxidation to form the mixed valence Ni(II,III) species. The voltammogram of the Cu(II) complex shows only a single reduction peak Cu(II)/ Cu(I) at -0.316 V during cathodic potential scan, whereas during the anodic potential scan, just after the reduction peak, an anodic peak is observed at 0.100 V. The separation between the peak potentials ($\Delta E_P = 416$ mV) indicates a quasi-reversible redox process and the ratio of peak current ≈ 1 corresponding to a simple one electron process (Shirin and Mukherjee, 1992) assignable to the Cu(II)/Cu(I) couple. The neutral uncomplexed ligand is proved not be electroactive over the range -0.8 to $+0.8$ V.

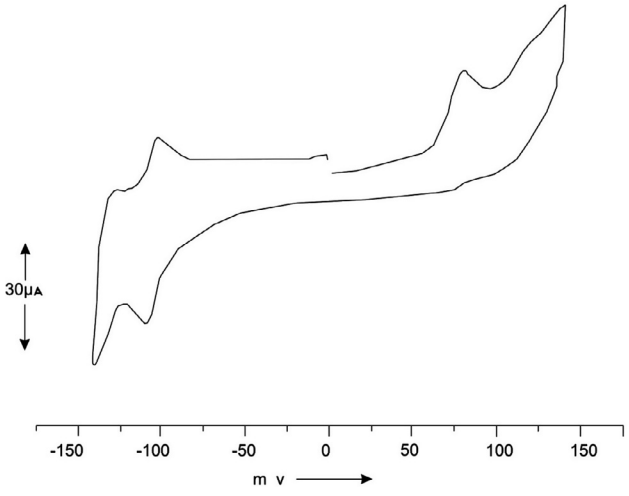

Figure 5 Cyclic voltammogram of complex I.

The voltammogram of the complex shows a cyclic oxidation–reduction process that does not change after repeated scans. This result may be explained by the stability of the process. The result indicates the effect of substitution of the Schiff base moiety on the electrochemical behavior for different complexes. The pyrrole ring stabilizes the M(II) in different complexes. This is possibly because the pyrrole ring makes the complex more positively charged and causes it to be more easily reduced.

Table 3 Crystallographic data of the complexes.

Complexes	Complex I	Complex III	Complex IV
Formula weight	358.17	391.06	413.91
Temperature (K)	298	298	298
Wave length (Å)	1.54056	1.54056	1.54056
Crystal system	Monoclinic	Triclinic	Triclinic
Space group	C 2/c	P_1	P_1
2θ range	10–70°	10–70°	10–70°
Unit cell dimensions (Å)	$a = 6.397563$	$a = 11.581102$	$a = 7.089919$
	$b = 6.460189$	$b = 11.905705$	$b = 8.763800$
	$c = 15.43264$	$c = 16.567397$	$c = 12.380807$
	$\alpha = \gamma = 90°$	$\alpha = 101.1729°$	$\alpha = 69.3141°$
	$\beta = 109.6280°$	$\beta = 101.3602°$	$\beta = 72.2471°$
		$\gamma = 115.8033°$	$\gamma = 104.1479°$
Volume (A^3)	2897.57	1910.47	630.23
Limiting indices	$-21 \leqslant h \leqslant 34$	$-3 \leqslant h \leqslant 3$	$-4 \leqslant h \leqslant 4$
	$-12 \leqslant k \leqslant 13$	$-3 \leqslant k \leqslant 3$	$-4 \leqslant k \leqslant 4$
	$-14 \leqslant l \leqslant 12$	$0 \leqslant l \leqslant 5$	$0 \leqslant l \leqslant 6$
Density (g/cc^3)	1.595	1.321	1.088
Z	8	4	1
Particle size (nm)	7.14	8.25	0.8112

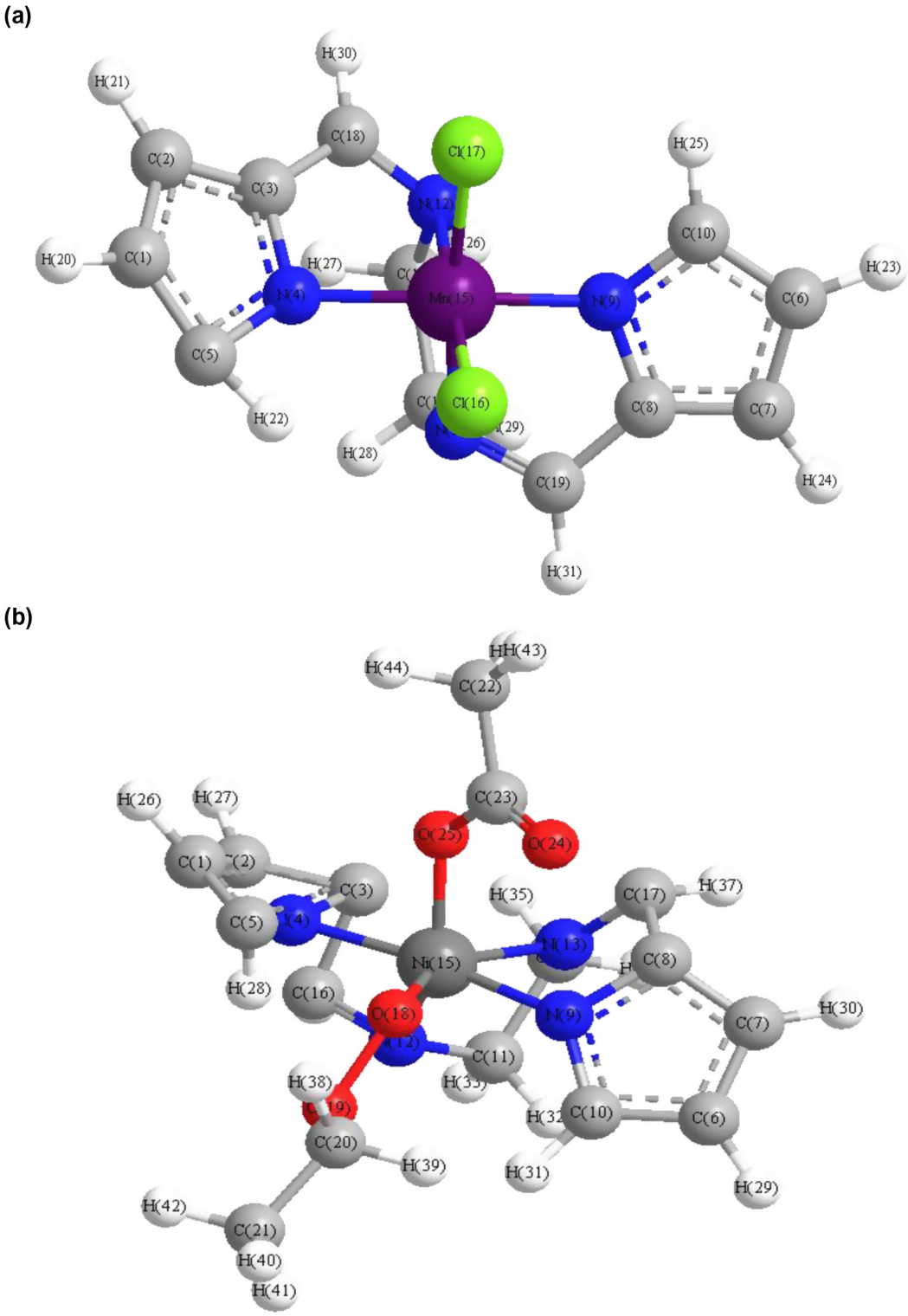

Figure 6 (a) Optimized structure of complex I. (b) Optimized structure of complex III.

3.3. Powder X-ray diffraction studies

In the absence of single crystal, X-ray powder data are especially useful to deduce accurate cell parameters. The diffraction pattern reveals the crystalline nature of the complex. The indexing procedures were performed using (CCP_4, UK) Crysfire program (Shirley, 2002) giving different crystal systems with varying space groups. The density and particle size of the metal complexes have been calculated. The cell parameters of the complexes are shown in Table 3. The crystal

Table 4 The prominent Bond length and bond angles of the metal complexes.

Complexes	Bond length(Å)	Bond angles	
I	Mn(15)–Cl(17): 2.1731	Cl(17)–Mn(15)–Cl(16)	86.5546
	Mn(15)–Cl(16): 2.1767	Cl(17)–Mn(15)–N(13)	172.8563
	N(9)–Mn(15): 1.8562	Cl(17)–Mn(15)–N(12)	91.3585
	N(4)–Mn(15): 1.8736	Cl(17)–Mn(15)–N(9)	92.1775
	N(12)–Mn(15): 1.8639	Cl(17)–Mn(15)–N(4)	94.2230
	N(13)–Mn(15):1.8695	Cl(16)–Mn(15)–N(13)	88.9302
		Cl(16)–Mn(15)–N(12)	177.6733
		Cl(16)–Mn(15)–N(9)	91.0310
		Cl(16)–Mn(15)–N(4)	96.7458
		N(13)–Mn(15)–N(12)	93.0468
		N(13)–Mn(15)–N(9)	82.3639
		N(13)–Mn(15)–N(4)	91.8010
		N(12)–Mn(15)–N(9)	88.0183
		N(12)–Mn(15)–N(4)	84.4255
		N(9)–Mn(15)–N(4)	170.2028
		C(19)–N(13)–Mn(15)	112.2833
		Mn(15)–N(13)–C(14)	110.2511
		C(18)–N(12)–Mn(15)	108.6978
		C(18)–N(12)–C(11)	107.0243
		Mn(15)–N(12)–C(11)	109.9465
II	Co(15)–O(18):1.8145	O(22)–Co(15)–O(18)	79.8019
	Co(15)–O(22):1.8145	O(22)–Co(15)–N(13)	80.0265
	N(9)–Co(15):1.8470	O(22)–Co(15)–N(12)	161.3773
	N(4)–Co(15):1.8512	O(22)–Co(15)–N(9)	106.9111
	N(12)–Co(15):1.8536	O(22)–Co(15)–N(4)	87.4329
	N(13)–Co(15):1.8520	O(18)–Co(15)–N(13)	153.9250
		O(18)–Co(15)–N(12)	114.5760
		O(18)–Co(15)–N(9)	84.1803
		O(18)–Co(15)–N(4)	81.3543
		N(13)–Co(15)–N(12)	88.9328
		N(13)–Co(15)–N(9)	86.0563
		N(13)–Co(15)–N(4)	114.0209
		N(12)–Co(15)–N(9)	87.0509
		N(12)–Co(15)–N(4)	83.4062
		N(9)–Co(15)–N(4)	157.4763
		C(17)–N(13)–Co(15)	104.2482
III	N(9)–Ni(15):1.8533	C(23)–O(25)–Ni(15)	127.0684
	N(4)–Ni(15):1.8845	O(19)–O(18)–Ni(15)	117.3006
	N(12)–Ni(15):1.8527	O(25)–Ni(15)–O(18)	96.1428
	N(13)–Ni(15):1.8583	O(25)–Ni(15)–N(13)	91.3438
	Ni(15)–O(18):1.8137	O(25)–Ni(15)–N(12)	141.7198
	Ni(15)–O(25):1.8032	O(25)–Ni(15)–N(9)	102.3075
		O(25)–Ni(15)–N(4)	79.7685
		O(18)–Ni(15)–N(13)	141.1931
		O(18)–Ni(15)–N(12)	113.8447
		O(18)–Ni(15)–N(9)	71.4448
		O(18)–Ni(15)–N(4)	97.0783
		N(13)–Ni(15)–N(12)	80.1331
		N(13)–Ni(15)–N(9)	69.7548
		N(13)–Ni(15)–N(4)	121.7281
		N(12)–Ni(15)–N(9)	109.2743
		N(12)–Ni(15)–N(4)	73.6450
		N(9)–Ni(15)–N(4)	168.4469
		C(17)–N(13)–Ni(15)	113.2010
		Ni(15)–N(13)–C(14)	120.3876
		C(16)–N(12)–Ni(15)	102.8050
IV	N(9)–Cu(15):1.9428	O(22)–Cu(15)–O(21)	71.7041
	N(4)–Cu(15):1.8797	O(22)–Cu(15)–N(13)	164.9179
	N(12)–Cu(15):1.3443	O(22)–Cu(15)–N(12)	79.8539
	N(13)–Cu(15):1.5871	O(22)–Cu(15)–N(9)	82.1779
	Cu(15)–O(21):1.8012	O(22)–Cu(15)–N(4)	95.3364

(*continued on next page*)

Table 4 (*Continued*)

Complexes	Bond length(Å)	Bond angles	
	Cu(15)–O(22):1.8124	O(21)–Cu(15)–N(13)	119.5691
		O(21)–Cu(15)–N(12)	151.0307
		O(21)–Cu(15)–N(9)	80.2377
		O(21)–Cu(15)–N(4)	87.5391
		N(13)–Cu(15)–N(12)	89.3995
		N(13)–Cu(15)–N(9)	89.7358
		N(13)–Cu(15)–N(4)	95.1684
		N(12)–Cu(15)–N(9)	101.5820
		N(12)–Cu(15)–N(4)	89.7643
		N(9)–Cu(15)–N(4)	167.7015
		O(22)–Cu(15)–O(21)	71.7041
		O(22)–Cu(15)–N(13)	164.9179
		O(22)–Cu(15)–N(12)	79.8539
		O(22)–Cu(15)–N(9)	82.1779
		O(22)–Cu(15)–N(4)	95.3364
		O(21)–Cu(15)–N(13)	119.5691
		O(21)–Cu(15)–N(12)	151.0307
		O(21)–Cu(15)–N(9)	80.2377
		O(21)–Cu(15)–N(4)	87.5391
		N(13)–Cu(15)–N(12)	89.3995
		N(13)–Cu(15)–N(9)	89.7358
		N(13)–Cu(15)–N(4)	95.1684
		N(12)–Cu(15)–N(9)	101.5820
		N(12)–Cu(15)–N(4)	89.7643
		N(9)–Cu(15)-N(4)	167.7015

data for complex I: monoclinic, space group C 2/c, $a = 6.397563$ Å, $b = 6.460189$ Å, $c = 15.43264$ Å, $V = 2897.57$ A^3, $Z = 8$, crystal data for complex III: triclinic, space group P_1, $a = 11.581102$ Å, $b = 11.905705$ Å, $c = 16.567397$ Å, $V = 1910.47$ A^3, $Z = 4$, crystal data for complex IV: triclinic, space group P_1, a = 7.089919 Å, $b = 8.763800$ Å, $c = 12.380807$Å, $V = 630.23$ A^3, $Z = 1$.

3.4. Molecular modeling studies

Molecular mechanics attempts to reproduce molecular geometries, energies and other features by adjusting bond length, bond angles and torsion angles to equilibrium values that are dependent on the hybridization of an atom and its bonding scheme. In order to obtain estimates of structural details of

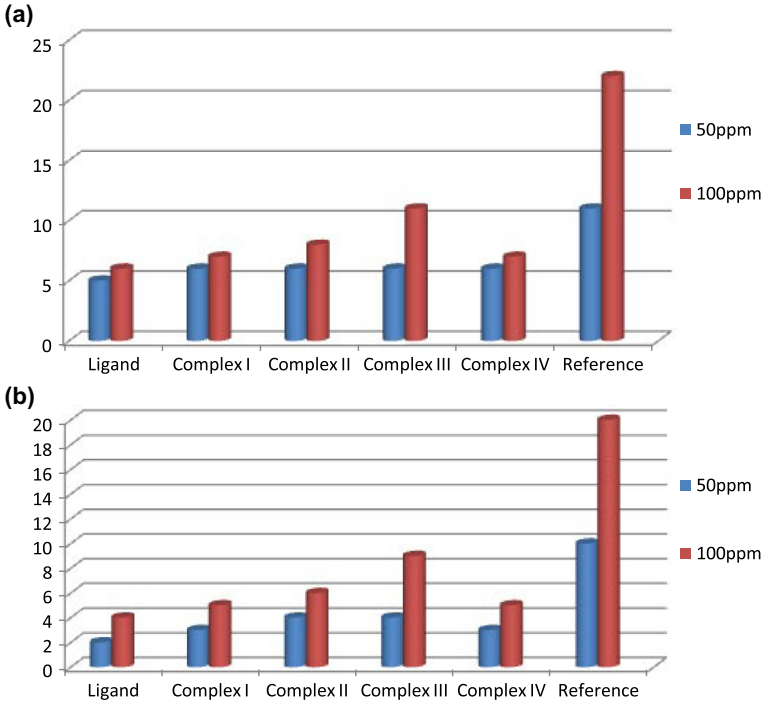

Figure 7 (a) Effect of different concentrations of ligand and complexes with *Escherichia coli*. (b) Effect of different concentrations of ligand and complexes with *Staphylococcus aureus*.

these complexes, we have optimized the molecular structure of complexes. Energy minimization was repeated several times to find the global minimum. The energy minimization value for octahedra without restricting the structure for the metal complexes is almost same. The energy minimization values for Complex I, II, III and IV are 85.37, 79.28, 107.97 and 55.76 kcal/mol, respectively. The copper complex has minimum energy whereas nickel complex has maximum energy. It indicates that the copper complex has maximum stability compared to other metal complexes. The optimized structure of metal complexes is shown in Fig. 6a and b and their prominent bond length and angles are represented in Table 4.

3.5. Biological studies

The bacteriological effect of the Schiff base and its metal complexes were determined against two bacteria under different concentration. The agar well – diffusion method was employed for the bacteria with respect to chloramphenicol as standard drug. The results showed that some compounds are very effective on some microorganisms (Fig. 7a and b). The nickel complex showed better activity than other metal complexes for both microorganisms. The activity of any compound is a complex combination of steric, electronic and pharmacokinetic factors. A possible explanation for the toxicity of the complexes has been postulated in the light of chelation theory. It was suggested that chelation considerably reduces the charge of the metal ion mainly because of partial sharing of its positive charge with the donor groups and possible π-electron delocalization over the whole chelate ring. This increases the lipophilic character of the metal chelate which favors its permeation through lipoid layers of cell membranes. Furthermore, the mode of action of the compounds may involve the formation of a hydrogen bond through – N═C group of the chelate or the ligand with the active centers of the cell constituents resulting in interference with the normal cell process. The higher bacteriotoxicity experienced by the compounds may be ascribed to the fact that the metal ions are more susceptible toward the bacterial cells than ligands (Phaniband and Dhumwad, 2007).

On the basis of above studies, geometries of the newly synthesized compounds have been proposed (Fig. 8). Metal complexes were found to be monomers and involved coordination through the azomethine nitrogen atoms, pyrrole nitrogen atoms and anions, giving octahedral geometry. The cell parameters of the complexes have been determined with the help of powder X-rays diffraction method. Bio-efficacy of the ligand and their metal complexes has been examined.

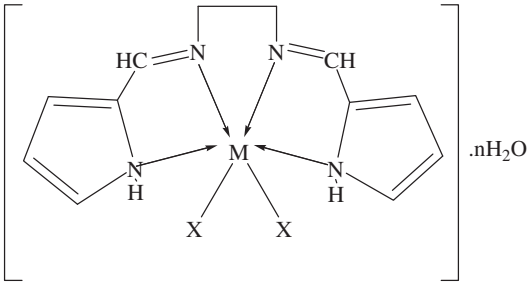

I M= Mn, X = Cl, n = 1
II M= Co, X = NO_3, n = 1
III M= Ni, X = CH_3COO, n = 0
IV M=Cu, X = CH_3COO, n = 1

Figure 8 Proposed structure of the complex.

Acknowledgment

Authors thankfully acknowledge Council of Scientific and Industrial Research (CSIR) and University Grants Commission (UGC) New Delhi, India for financial assistance.

References

Abd El-Wahab, Z.H., El-Sarrag, M.R., 2004. Spectrochim. Acta A 60, 271.
Addision, C.C., Logan, N., Wallwork, S.C., Garner, C.D., 1971. Quart. Rev. Chem. Soc. 25, 289.
Addison, C.C., Sultons, D., 1967. Prog. Inorg. Chem. 8, 195.
Ahamed, T., Nishat, N., Parveen, S., 2008. J. Coord. Chem. 61 (12), 1963.
Alvarez, C.M., Garcia-Rodriguez, R., Miguel, D., 2007. Dalton Trans. 32, 3546.
Anacona, J.R., Marquez, V.E., Jimenez, Y., 2009. J. Coord. Chem. 62 (7), 1172.
Aranha, P.E., DosSantos, M.P., Romera, S., Dockal, E.R., 2007. Polyhedron 26, 1373.
Belaid, S., Landreau, A., Djebbar, S., Benali-Baitich, O., Khan, M.A., Bouet, G., 2008. J. Inorg. Biochem. 102, 63.
Beloso, I., Castro, J., Garcia-Vazquez, J.A., Perez- Lourido, P., Romero, J., Sousa, A., 2003. Polyhedron 22, 1099.
Berube, C.D., Gambarotta, S., Yap, G.P.A., Cozzi, P.G., 2003. Organometallics 22, 434.
Bew, M.J., Hathaway, B.J., Fereday, R.J., 1972. J. Chem. Soc., Dalton Trans., 1229.
Bezaatpour, A., Amiri, M., Jahed, V., 2011. J. Coord. Chem. 64 (10), 1837.
Carlin, R.L., 2002. Magnetochemistry. Springer-Verlag, New York [41A, 1821].
Chandra, S., Sharma, S.D., 2002. Trans. Met. Chem. 27, 732.
Choca, M., Ferraro, J.R., Nakamoto, K., 1972. J. Chem. Soc. A, 2297.
Cotton, F.A., Wilkinson, G., 1972. Advance Inorganic Chemistry, third ed. Wiley Eastern Ltd.
Figgis, B.N., 1978. Introduction to Ligand Field Theory. Wiley-Interscience, New York.
Figgis, B.N., Lewis, J., 1964. Prog. Inorg. Chem. 37, 37.
Firdaus, F., Fatma, K., Azam, M., Shakir, M., 2010. J. Coord. Chem. 63 (22), 3956.
Gudasi, K.B., Patil, M.S., Vadavi, R.S., Rashmi, V.S., Patil, S.A., 2006. Trans. Met. Chem. 31, 580.
Hathaway, B.J., Billing, D.E., 1970. Coord. Chem. Rev. 5, 143.
Jorgensen, C.K., 1969. Oxidation Numbers and Oxidation States. Springer, New York, p. 106.
Kandaz, M., Coruhlu, S.Z., Yilmaz, I., Ozkaya, A.R., 2002. Trans. Met. Chem. 27, 877.
Kasumov, V.T., Ozalp-Yaman, S., Tas, E., 2005. Spectrochim. Acta A 62, 716.
Keypour, H., Rezaeivala, M., Valencia, L., Salehzadeh, S., Perez-Lourido, P., Khavasi, H.R., 2009. Polyhedron 28, 3533.
Kivelson, D., Neiman, R.R., 1968. J. Chem. Soc. A, 1678.
Kumar, D.N., Singh, B.K., Garg, B.S., Singh, P.K., 2003. Spectrochim. Acta A 59, 1487.
Kumar, D.S., Alexander, V., 1999. Polyhedron 18, 1561.
Kumar, R., Chandra, S., 2007. Spectrochim. Acta A 67, 188.
Lever, A.B.P., 1984. Inorganic Electronic Spectroscopy, second ed. Elsevier, Amsterdam.

Lever, A.B.P., Manto Vani, E., Ramaswami, B.S., 1971. Can. J. Chem. 49, 1957.
Mohamed, G.G., Omar, M.M., Hindy, A.M.M., 2005. Spectrochim. Acta A 62, 1140.
Nakamoto, K., 1978. Infrared and Raman Spectra of Inorganic and Coordination Compounds. Wiley, New York.
Omar, M.M., Mohamed, G.G., 2005. Spectrochim. Acta A 61, 929.
Parekh, H.M., Patel, M.N., 2006. Russ. J. Coord. Chem. 32 (6), 431.
Phaniband, M.A., Dhumwad, S.D., 2007. Trans. Met. Chem. 32, 1117.
Prakash, A., Singh, B.K., Bhojak, N., Adhikari, D., 2010. Spectrochim. Acta A 76, 356.
Raman, N., Sakthivel, A., Rajasekaran, K., 2009. J. Coord. Chem. 62 (10), 1661.
Ramesh, R., Maheshwaran, S., 2003. J. Inorg. Biochem. 96, 457.
Ranford, J.D., Sadler, P.J., Tocher, D.A., 1993. J. Chem. Soc., Dalton Trans., 3393.
Ray, A., Banerjee, S., Butcher, R.J., Desplanches, C., Mitra, S., 2008. Polyhedron 27, 2409.
Saleh, A.A., 2005. J. Coord. Chem. 58 (3), 255.
Sanmartin, J., Novio, F., Garcia-Deibe, A.M., Fondo, M., Ocampo, N., Bermejo, M.R., 2006. Polyhedron 25, 1714.
Shirin, Z., Mukherjee, R.M., 1992. Polyhedron 11, 2625.
Shirley, R., 2002. The CRYSFIRE System for Automatic Powder Indexing: Users Manual. Lattice Press.
Silverstein, R.M., Webster, F.X., 2007. Spectrometric Identification of Organic Compounds, sixth ed. Wiley, India.
Singh, B.K., Prakash, A., Adhikari, D., 2009. Spectrochim. Acta A 74, 657.
Singh, B.K., Prakash, A., Rajour, H.K., Bhojak, N., Adhikari, D., 2010. Spectrochim. Acta A 76, 376.
Swamy, S.J., Pola, S., 2008. Spectrochim. Acta A 70, 929.
Tomilson, A.A.G., Hathaway, B.J., Billing, D.E., Nicholls, P., 1965. J. Chem. Soc. A, 65.
Uysal, S., Kursunlu, A., 2011. J. Inorg. Organomet. Polymer Mater. 21 (2), 291.
Valencia, L., Adams, H., Bertolo, E., Macias, A., Rodriguez, A., 2001. Inorg. Chim. Acta 317, 45.
Wang, Q.L., Zhao, B., Liao, D.Z., Yan, S.P., Cheng, P., Ziang, Z.H., 2003. Trans. Met. Chem. 28, 326.
Yang, G., Liu, M., Li, X., Li, J., Ma, J., 2009. J. Coord. Chem. 62 (21), 3478.
Yilmaz, I., Gurek, A.G., Ahsen, V., 2005. Polyhedron 24, 791.
Yilmaz, I., Kocak, M.B., 2004. Polyhedron 23, 1279.
Yoshida, N., Ichikawa, K., Shiro, M., 2000. J. Chem. Soc., Perkin. Trans. 2, 17.